Transmembrane distribution of kanamycin and chloramphenicol: insights into the cytotoxicity of antibacterial drugs†

Chao Song, Nai-Yun Gao and Hong-Wen Gao*

Received 21st October 2009, Accepted 19th April 2010
DOI: 10.1039/b921810f

Antibiotics are widely used and their abuse has caused ecological hazard. Recently, pollution from pharmaceuticals and personal care products (PPCPs) has aroused great concern among governments and researchers. In order to elucidate the correlations among molecular structure, transmembrane distribution and toxicological effects of different kinds of antibiotics, zebrafish (*Danio rerio*) embryos and larvae were exposed to two structurally different antibiotics, kanamycin (KAN) and chloramphenicol (CAP). The membrane distribution and toxicological effects of these antibiotics were investigated. The association of KAN with the embryos fitted a general Langmuir isotherm and was attributed to electrostatic attraction and hydrogen bond formation. The saturation number of KAN is 252 ± 13 nmol per embryo and the adsorption constant (5.24 ± 0.05) × 10^3 L mol^{-1}. The interaction of CAP with the embryos conformed to a general model of partitioning behavior with the partition coefficient being 14.20 ± 0.94 μL per embryo, and was attributed to hydrophobic effects. More than 89% of the adsorbed KAN was located on the outer surface of the embryonic chorion, but over 80% of the adsorbed CAP entered the internal matrix. High antibiotic concentrations were lethal to most embryos, while low concentrations were teratogenic. KAN and CAP had different transmembrane distribution and their toxicities differed in character. KAN mainly accumulated on the outer membrane caused *e.g.* axial malformation (AM). In contrast, CAP readily went through the membrane into the cytoplasm and caused *e.g.* serious pericardial edema (PE), yolk sac edema (YSE) and hemagglutination (HE). The new method could be useful for evaluating the interactions of toxins with membranes and elucidating the mechanisms of cytotoxicity.

Introduction

Antibiotics are often used to control human and animal diseases. Since the 1990s, they have also played an important role as growth promoters in stock farming and aquiculture.[1–3] More than 1300 kinds of new drugs are produced annually in China, and 70% of these are antibiotics, with an annual yield of 33 000 ton. However, the abuse of antibiotics and illegal discharge of drug plant wastewater has caused serious losses in recent decades, especially in developing countries. In addition, antibiotics are not completely absorbed by humans and animals,[4,5] so large quantities enter various parts of the environment as waste. As exogenous chemicals, they may damage the ecological environment[2,6,7] and further affect people's lives and health. Increasing attention has recently been focused on the probable environmental risks and ecological hazards from antibiotics and pharmaceuticals and personal care products (PPCPs).[8,9] More than 50 kinds of PPCPs have been detected in various environmental samples, animal tissues and human blood. Also, gender disorders in fish and teratogenesis in frogs have been observed in water bodies polluted by wastewater from drug-manufacturing plants. With a few exceptions, which cause acute poisoning, most drug residues lead to chronic and cumulative toxicity *e.g.* carcinogenicity, mutagenicity, neurotoxicity and teratogenicity.[10–12] For example, erythromycin, tetracycline and rifampicin have hepatotoxic effects. Studies of their toxic effects on animal development and growth have focused on mammals *e.g.* mice,[13,14] cows[15] and rabbits,[16] and on birds[17] and amphibians such as frogs.[18]

Kanamycin sulfate (KAN), as a kind of aminoglycoside antibiotic, is soluble and stable in water, has low bacterial resistance and low cost, and can be administered both orally and intravenously.[19] Such antibiotics have been in common use for a wide variety of infectious diseases caused by Gram-negative and Gram-positive bacteria.[20,21] However, they have adverse effects, causing serious ototoxicity and nephrotoxicity.[22–24] The use of aminoglycoside antibiotics has declined in many countries, but they are still in common use in developing countries.[24] Chloramphenicol (CAP) is a broad-spectrum antibiotic that inhibits a variety of aerobic and anaerobic microorganisms.[25] It is highly effective in agricultural, veterinary and aquaculture practice,[26–28] but it causes many adverse effects such as bone marrow suppression,[29–31] aplastic anemia,[32,33] leukemia[34] and gray baby syndrome.[35] Bone marrow hematopoiesis is impaired when more than 1 mg kg^{-1} CAP remains in animal tissues. In addition, it is toxic to nerves and kidneys, and humans are

State Key Laboratory of Pollution Control and Resources Reuse, College of Environmental Science and Engineering, Tongji University, Shanghai, 200092, China. E-mail: hwgao@tongji.edu.cn; Fax: +86 (021) 65988598; Tel: +86 (021) 65988598
† Electronic supplementary information (ESI) available: Text containing eqn (S1) to (S2) and Fig. S1 to S8. See DOI: 10.1039/b921810f

more sensitive to its effects than other animals. Owing to resistance and safety concerns, consumption of CAP has been restricted by most countries.[3] Nevertheless, it is still illegally used by farmers and aquaculturists,[25] because it is exceedingly inexpensive and readily available.

There have been increasing numbers of reports about the ecotoxicological effects of these two kinds of antibiotics.[36–38] Obviously, any chemical that affects the function of a target biomolecule causes toxicity only when it penetrates the cell, must first cross the cell membrane.[39] The toxicity-causing mechanisms of exogenous chemicals have been elucidated but they often focus on the interactions with target molecules,[40–45] errors in protein expression,[46] alteration of gene sequences[38] and dose-effect relationships.[28,47] In this study, zebrafish (*Danio rerio*) embryos were exposed to KAN and CAP, which differ markedly in structure and polarity, as representative antibiotics. The zebrafish is an ideal model for investigating developmental toxicity in vertebrates at an early life stage (ELS).[48,49] The aim of this work was to elucidate the potential mechanisms of cytotoxicity of typical antibiotics by investigating their interactions with embryos and then revealing their membrane transport pathways.

Results and discussion

Interactions of KAN and CAP with phosphatidylcholine

Lecithin (phosphatidylcholine) occurs in all cellular organisms, being one of the typical composition of the phospholipid portion of the cell membrane and single membrane liposome (SML) prepared by dispersing lecithin into suspension are often used to simulate the phospholipid membrane.[39] The components in the commercial lecithin were detected to contain 95.4% ± 0.6% phosphatidylcholine (PC), 3.0% ± 0.2% phosphatidylethanolamine (PEA) and 1.6% ± 0.5% palmitic acid triglyceride (TP) (ESI†, Fig. S1).[50] By the HPLC determination of the unreacted KAN and CAP concentrations free in their SML-mixing liquids (ESI†, Fig. S2), the associations of KAN and CAP with SML approached equilibrium within 1 h (ESI†, Fig. S3A). The amount (γ) of KAN bound to the lecithin increased with increasing the initial concentration (c_0) and it approached a constant maximum at more than 0.5 mM KAN (Fig. 1A–1). According to the molecular structure of KAN sulfate (ESI†, Fig. S2A), the $-NH_3^+$ group positively charged may bind to the $>PO_4^-$ heads of PC and PEA (structured in ESI†, Fig. S1B) by the electrostatic attraction, where the fraction of KAN binding to PEA of lecithin is much less than that to PC. The interaction is similar to the aggregation of cationic compound on anionic surfactant micelle.[51] The general Langmuir isotherm model (ESI†, eqn (S1))[52] was used to fit the experimental data as illustrated in Fig. 1B–3. In view of the good linearity, the binding of KAN obeyed the monolayer adsorption. From the regression line of plots γ^{-1} *vs.* $c_L{}^{-1}$ (Fig. 1B–3), a slope and an intercept were calculated. The saturated adsorption mole number (N) of KAN was calculated to be 0.19 ± 0.01 mole per mole PC, *i.e.* one KAN molecule bound to approximately five PC molecules. The binding constant (K) of KAN was calculated to be (8.03 ± 0.01) × 10^3 L mol^{-1}.

In contrast, CAP binding to SML increased linearly with increasing c_0 of CAP (Fig. 1A–2). From plots $[CAP]_{PC}$ *vs.* $[CAP]_{water}$, the slope $[CAP]_{PC}/[CAP]_{water}$ *i.e.* partition constant ($P_{PC/water}$) (ESI†, eqn (S2)) was calculated as given in Fig. 1B–4. The good linear relationship indicates that the binding of CAP to SML obeyed the lipid–water partition law.[53] Thus, the more CAP is added and the more CAP binds to SML. The $P_{PC/water,CAP}$ of CAP was calculated to be 122 ± 15 L kg^{-1} (Fig. 1B–4) *i.e.* log P = 1.28. The CAP belongs to hydrophobic substance (ESI†, Fig. S2B), where it contains two hydrophobic groups,[54] nitrophenyl (log P = 1.89) and dichloromethyl (log P = 1.18). Thus, it may enter the long aliphatic chain region of lecithin by hydrophobic effects.

Effects of electrolyte, pH and temperature on KAN/CAP–SML interactions

Fig. 2 shows the effects of ionic strength, pH and temperature on γ_{KAN} of KAN and $[CAP]_{PC}$ of CAP bound to the SML. γ_{KAN} increased markedly with increasing ionic strength (Fig. 2A–1). Similar to dipalmitoylphosphatidylcholine (DPPC) multilayers, the packing density of the PC molecules in the SML bilayer and the molecular order degree increased in the presence of salt due to screening effects by Cl^- ions with consequent reduction of the electrostatic repulsion between polar heads.[55] This means that there are more PC molecules packing in the SML bilayer and the KAN cations are more favorably bound to SML. In addition, a great deal of Cl^- tended to adsorption to the zwitterionic headgroup dipoles[56,57] to form an anion layer which is favorable for the binding of KAN cations. On the other hand, increasing salt concentration decreased the activity coefficient of solvent and then drove KAN to partition more readily into non-aqueous phase. From Fig. 2B–1, there was no significant difference of γ_{KAN} between pH 4.5 and 8.5. According to pK_a values of phosphocholine (approx. 0.8)[58] and KAN (more than 8),[59] the ions: $>PO_4^-$ in PC and $-NH_3^+$ in KAN are predominant within such a pH scope. From Fig. 2C–1, γ_{KAN} increased obviously with the increase of temperature before 40 °C. From plots ln K *vs.* T^{-1} fitted the van't Hoff equation (Fig. 3),[60] the entropy change (ΔS) was calculated to be 128.0 ± 15.3 J mol^{-1} K^{-1} and the enthalpy change (ΔH) to be +(20.8 ± 4.6) kJ mol^{-1}. The free enthalpy (ΔG) is less than zero and the KAN–SML interaction is spontaneous which was driven by entropy increase. The endothermic reaction indicated that a higher temperature favored the KAN binding to SML. γ_{KAN} reached the equilibrium after 45 °C (Fig. 2C–1). The possible reason is due to the phase transition of PC.[57] In contrast, the effects of pH, ionic strength and temperature on $[CAP]_{PC}$ are not obvious (Fig. 2A–C–2). It may be attributed to the fact that the hydrophobic effects were seldom influenced.

Association of KAN and CAP with embryos

In order to investigate the effects of the antibiotics on embryonic development, five embryos were exposed to KAN (c_0, 0.100–1.70 mM) and CAP (c_0, 120–1280 mg L^{-1}). From the time experiment, KAN and CAP adsorption to the embryos reached equilibrium at 6 and 2 h, respectively (ESI†, Fig. S3 B). It is obviously different from the results of the

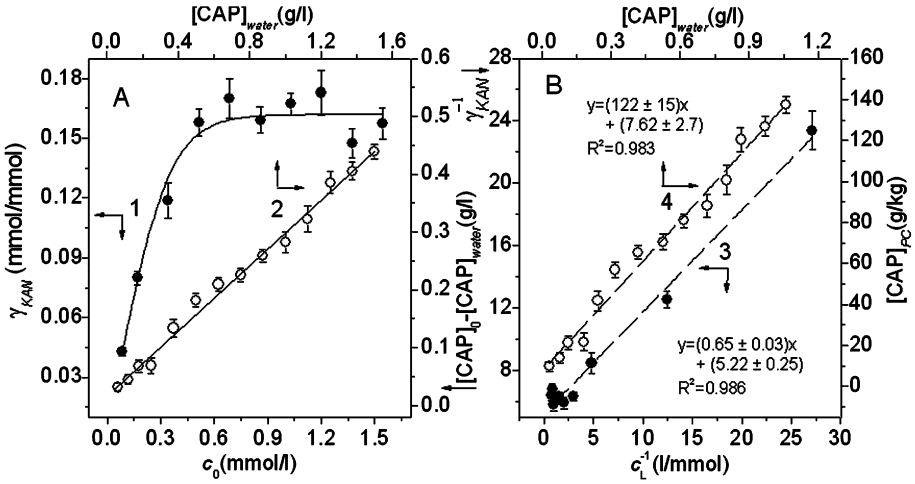

Fig. 1 The binding numbers (γ_{KAN}) of kanamycin sulfate (KAN) and the bound amount of CAP ($[CAP]_{PC}$) on single membrane liposome (SML) were calculated by determining the concentration of antibiotic remaining in the supernatant by high performance liquid chromatography (HPLC) after the KAN/CAP-PC mixture had been incubated for 1 h at 25 °C and centrifuged for 10 min at 12 000 rpm: A–B, KAN [initial exposure concentration (c_0) from 0.10 to 1.5 mM]; C–D, CAP [initial exposure concentration (c_0) from 60 to 1500 mg L^{-1})].

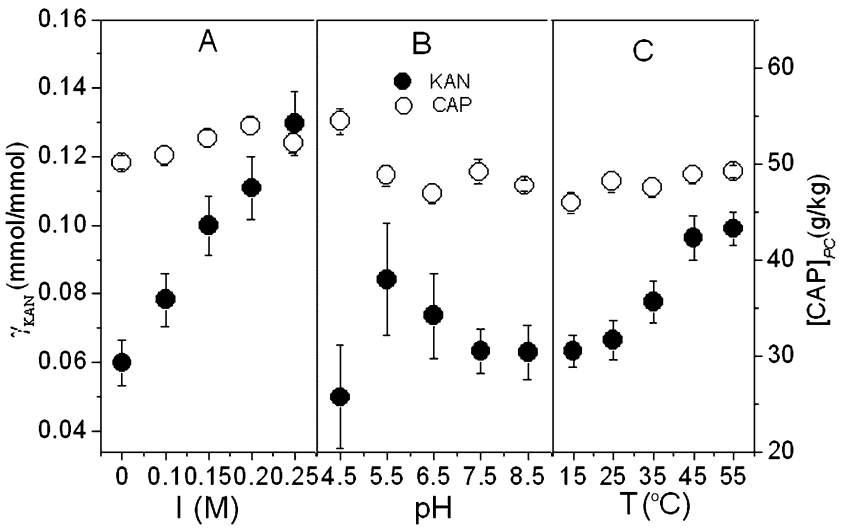

Fig. 2 Effects of ionic strength (A), pH (B) and temperature (C) on γ_{KAN} of KAN and $[CAP]_{PC}$ of CAP on SML: 1, 0.70 mM KAN; 2, 65 mg L^{-1} CAP.

in vitro experiment with SML (ESI†, Fig. S3A). The possible reason is that the growth and metabolism of the embryos affected the transport of the antibiotics. During the initial embryonic stage *i.e.* the first 6 h, the blastoderm cells become smaller as embryo cleavage continues. The cells become concentrated at one end of the oosphere and there is little structural and compositional difference among them. The amounts of KAN (γ_{KAN}) and CAP ($[CAP]_{embryo}$) adsorbed to the embryos were determined after 8 h exposure and the results are given in Fig. 4. γ_{KAN} approached a maximum when KAN is more than 1.2 mM (Fig. 4A). The data conformed to the general Langmuir adsorption isotherm (Fig. 4B; ESI†, eqn (S1)). The N of KAN was calculated to be 252 ± 13 nmol, *i.e.* 252 nmol of KAN bound to one embryo. The K of KAN was calculated to be (5.24 ± 0.05) × 10^3 L mol^{-1}, which approaches that obtained in the *in vitro* experiment with SML. Thus, KAN are mainly distributed on the membrane and attracted by the $>PO_4^-$ group of the membrane bilayer. Besides the typical lecithin composition, the small negative charges *e.g.* glutamic acid (Glu) residues, phosphoethanolamines and phosphoserines on membrane[61,62] may attract the KAN cation, too. In addition, a great deal of polar groups *e.g.* –COOH, –OH and $–NH_2$ on the membrane surface, probably interacted with KAN *via* hydrogen bonds and van der Waals forces. The combination of interactions/bonds would cause KAN to be adsorbed firmly on the outside surface of the membrane. In contrast, $[CAP]_{embryo}$ of CAP increased linearly with increasing c_0 (Fig. 4C), and the association of CAP conformed to a general model of partitioning behavior (Fig. 4D), similar to that with SML. The partition coefficient was calculated to be $P_{embryo/water,CAP}$ = 14.2 ± 0.9 μL per embryo, *i.e.* roughly 479 L kg^{-1}, which is much higher than that obtained in the *in vitro* SML experiment. The main reason may be that CAP entered the embryo cytoplasm. Besides,

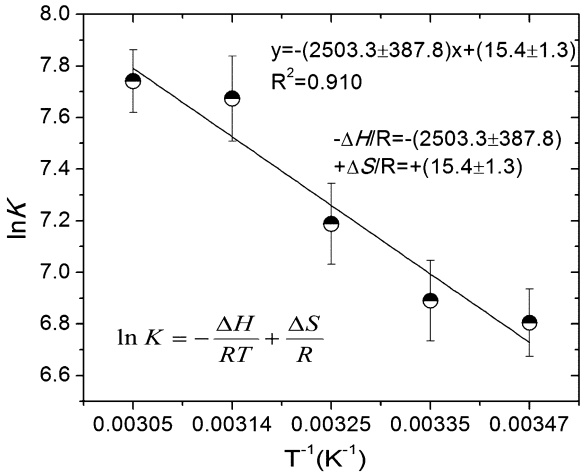

Fig. 3 Plots of ln K *vs.* T^{-1} for the KAN–SML interaction with the van't Hoff equation. T is the absolute T/K, R the gas constant being 8.314 J mol^{-1} K^{-1}, K equilibrium constant, ΔH enthalpy change (J mol^{-1}) and ΔS entropy change (J mol^{-1} K^{-1}). From the slope and the intercept of the linear regression plots ln K *vs.* T^{-1}, both ΔH and ΔS were calculated: $\Delta H = +(20.8 \pm 4.6)$ kJ mol^{-1} and $\Delta S = (128.0 \pm 15.3)$ J mol^{-1} K^{-1}. $\Delta G = \Delta H - T\Delta S$, were calculated to be $-(16.1 \pm 0.2)$ kJ mol^{-1} at 15 °C, $-(17.4 \pm 0.1)$ kJ mol^{-1} at 25 °C, $-(18.6 \pm 0.2)$ kJ mol^{-1} at 35 °C, $-(19.9 \pm 0.3)$ kJ mol^{-1} at 45 °C and $-(20.2 \pm 0.5)$ kJ mol^{-1} at 55 °C. All ΔG values are less than 0.

embryo membrane has a much more complicated structure than SML. Therefore, these two kinds of antibiotics have seriously different interactions with the embryos.

Ionic strength, pH and temperature affected the binding of KAN and CAP to the embryo (ESI†, Fig. S4). The γ_{KAN} of KAN increased with increase ionic strength. The possible reason is that the large amounts of Cl^- tended to adsorption to the outer surface of chorion[56,57] which is favorable for the binding of KAN. The pH does not have an obvious effect on γ_{KAN} and temperature. The amount ($[CAP]_{embryo}$) of CAP bound to the embryos increased and reached a maximum with increase of NaCl to 0.1 M. The $[CAP]_{embryo}$ decreased when the electrolyte concentration exceeded 0.1 M. It may be due to embryo activity weakening in a higher concentration of electrolyte. $[CAP]_{embryo}$ is not significantly affected by pH. The higher temperature is favorable for CAP binding to the embryos. A possible reason is that the membrane flow rate increased and metabolic activity accelerated at a higher temperature. $[CAP]_{embryo}$ increased rapidly at higher than 40 °C. This may be because the phase transition of membrane lipids occurred,[57] and the movement freedom of PC chains becomes greater.[60] Thus, CAP is more accessible through the membrane and combined with other lipids, such as the storage lipids in the cytoplasm. Therefore, the amount of CAP binding to embryo exhibited an obvious increase.

Transmembrane distribution of KAN and CAP

The cell membrane acts as a natural barrier and plays a protective role in normal cellular activity. The membrane consists of a phospholipid bilayer and membrane proteins along with oligosaccharides. It performs a number of essential functions such as nutrient transport, ion conduction, signal transduction, *etc.* Accumulation of any harmful chemical in the membrane may cause membrane expansion, blockage of the ion pumps and altered proton permeability.[62,63] Understanding transmembrane transport of chemicals is helpful for revealing the toxicity mechanism of a harmful chemical. The distributions of KAN and CAP were determined by fragmenting and separating the different parts of embryos (ESI†, Fig. S5). Most of the antibiotics remained in the extracellular medium

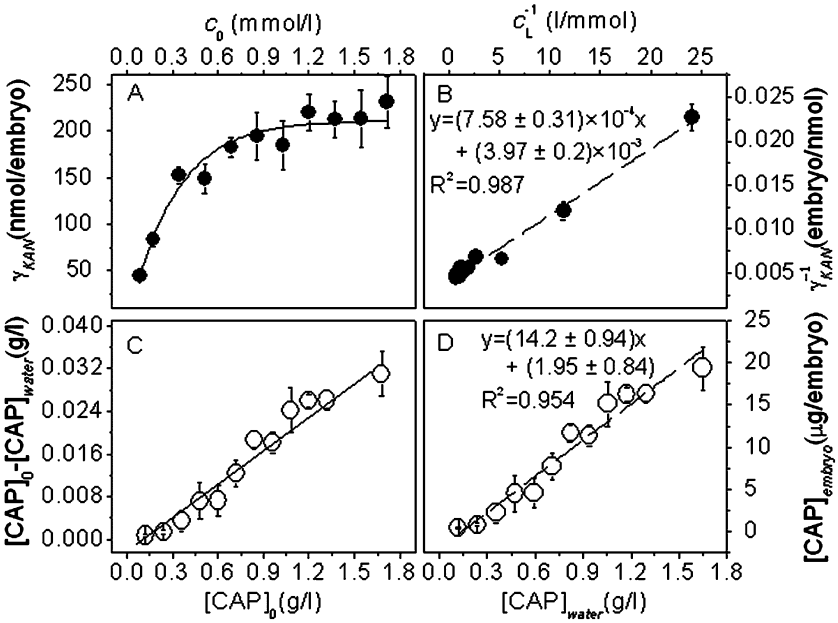

Fig. 4 The binding numbers (γ_{KAN}) of kanamycin sulfate (KAN) and the bound amount of chloramphenicol ($[CAP]_{embryo}$) on zebrafish embryos (n = 5) were calculated by measuring the concentration of antibiotic remaining in the supernatant (c_L) by high performance liquid chromatography (HPLC) after the embryos had been incubated with KAN/CAP for 8 h at 25 °C: A–B, KAN [initial exposure concentration (c_0): 0.10 to 1.7 mM]; C–D, CAP [initial exposure concentration (c_0): 120 to 1680 mg L^{-1}].

(Fig. 5). Over 89% of the adsorbed KAN was located on the membrane *i.e.* chorion and only a little amount of KAN entered the cytoplasm *i.e.* matrix inside the chorion. KAN is strongly hydrophilic and $-NH_3^+$ group of KAN is predominant in aqueous solution. Most of the adsorbed KAN was distributed on the membrane and only a small amount in the cytoplasm (Fig. 5A). The amount of CAP adsorbed on the embryos increased with increasing the exposure concentration (Fig. 5B). In contrast to KAN, over 80% of the adsorbed CAP was found in the cytoplasm and less than 20% distributed on the membrane. The distribution of CAP in different parts of embryos may be relevant to the different lipid composition in different parts, *i.e.* chorion is mainly composed of membrane lipids (phospholipids) and there are some storage lipids (in the yolk) in the cytoplasm. As the lipid–water partition coefficients for storage lipids were higher than that for phospholipids,[60] CAP was readily transported through the membrane into the cytoplasm. The 3D-morphology of the chorion surface showed that the exposure to KAN caused adhesion among the protuberances and obscured the lower membrane layer (ESI†, Fig. S6C). The association of KAN molecules with the outer membrane surface altered the membrane structure, which may affect the flow/rotation of phospholipids, transport of membrane proteins, import of necessary substances and export of metabolic wastes. However, the change in morphology in the CAP exposure group indicated the membrane surface became rough (ESI†, Fig. S6B). The average headgroup spacing increased with the thinning effect to the membrane[64] in comparison with the control sample (ESI†, Fig. S6A). Membrane thinning has been suggested as a possible mode of membrane disruption.[65] The highly hydrophobic CAP may insert easily into the bilayer hydrocarbon core and the disruption to lipid packing affect greatly the normal interactions of PC/PEA with the cytoskeletal proteins.

On the basis of the above data, CAP and KAN showed different distribution character, so they may have different transport pathways from the extra-embryonic medium to the developing cells, as illustrated in Fig. 6. For CAP, the first step is partitioning from the medium into the membrane phospholipid bilayer. Subsequently, owing to the activity and metabolism of the cells and the different lipid/water partition for different kinds of lipids,[60] CAP is readily transported through the membrane into the cytoplasm, which contains many storage lipids in the yolk of the embryo. This partitioning/reverse partitioning depends on the hydrophobic effects of CAP with the aliphatic chains of lipids (Fig. 6a). As a speculation, the transfer of CAP into the developing cells may cause chemical damage, *e.g.* marrow toxicity, the most serious manifestation of which is aplastic anemia.[31] In contrast, KAN was mainly adsorbed on the outer membrane surface (Fig. 6) *via* electrostatic attraction, hydrogen bond and van der Waals forces (Fig. 6b), but a little amount of KAN entered the cytoplasm. Thus, a high concentration of KAN may form an adhesion shell enclosing the membrane, leading to physical membrane damage, *e.g.* obstruction of extracellular signal transmission, impairment of membrane transport and asphyxiation of the cells.

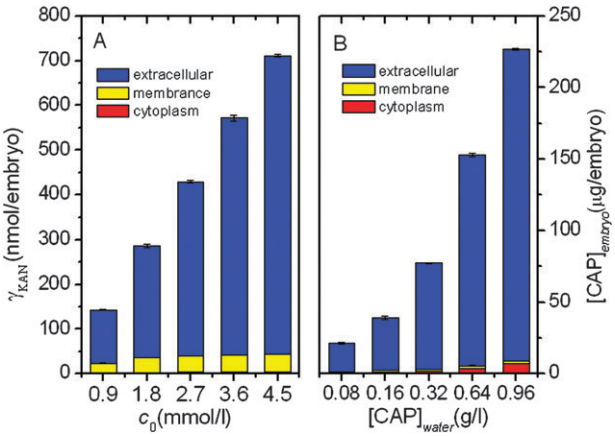

Fig. 5 The distribution of kanamycin sulfate (KAN) or chloramphenicol (CAP) in different parts (extracellular fluid, membrane and cytoplasm) of the zebrafish embryos (n = 8) was evaluated by determining the concentrations of KAN/CAP and calculating the binding numbers (γ_{KAN}) and the bound amount of chloramphenicol ([CAP]) in different parts of the embryos after incubation in KAN/CAP for 8 h at 25 °C: A, KAN [initial exposure concentration (c_0): 0.90, 1.8, 2.7, 3.6 and 4.5 mM]; B, CAP [initial exposure concentration (c_0): 0.08, 0.16, 0.32, 0.64 and 0.96 g L^{-1}].

Effects of KAN and CAP on the development of zebrafish embryos and larvae

From the photographs taken during zebrafish embryo development, most of the embryos hatched at 2 day post-fertilization (dpf) in the control group (Fig. 7A). In the KAN exposure group (Fig. 7B), none of the embryos hatched at 2 dpf and some hatched at 3 dpf with obviously axial malformation (AM) (Fig. 7B–3). KAN was mainly adsorbed on the outer chorion surface, perhaps affecting nutrient absorption, thus causing AM in the exposed embryos (Fig. 7B) and larvae (ESI†, Fig. S7A). In the CAP exposure group, just a few embryos hatched at 2 dpf with evident pericardial edema (PE) and hemagglutination (HE) (Fig. 7C–4). CAP passed readily through the chorion and transported into the developing embryonic cell, where it may disrupt oxidative phosphorylation[35] and reduce myocardial contractility[66] leading to ventricular dysfunction.[67] Thus, severe PE, yolk sac edema (YSE) and severe HE were found in the exposed embryos (Fig. 7C) and larvae (ESI†, Fig. S7B).

Fig. 8 shows the mortality rates of the embryos exposed to KAN and CAP. In the KAN exposure group, no embryos died before hatching (3 dpf) (Fig. 8A). Obvious acute toxicity appeared in more than 2.88 mM KAN, and chronic toxicity in less than 1.44 mM. All the embryos died in 5.76 mM KAN at 5th day, while only 20% died in 1.44 mM at 11st day (Fig. 8A). In contrast to the embryos, all larvae died in 5.76 mM KAN after only one day's exposure, while about 20% died in 1.44 mM after 7 days (ESI†, Fig. S8A). The embryos exihibited an obvious lethal effect in more than 0.24 mM CAP, and serious teratogenic effect in less than 0.12 mM (Fig. 8B). All embryos died in 0.48 mM CAP after one day's exposure but none of them died in less than 0.12 mM after 7 days. All larvae died in 0.96 mM CAP after one day's exposure but none died in 0.24 mM after 7 days (ESI†, Fig. S8B).

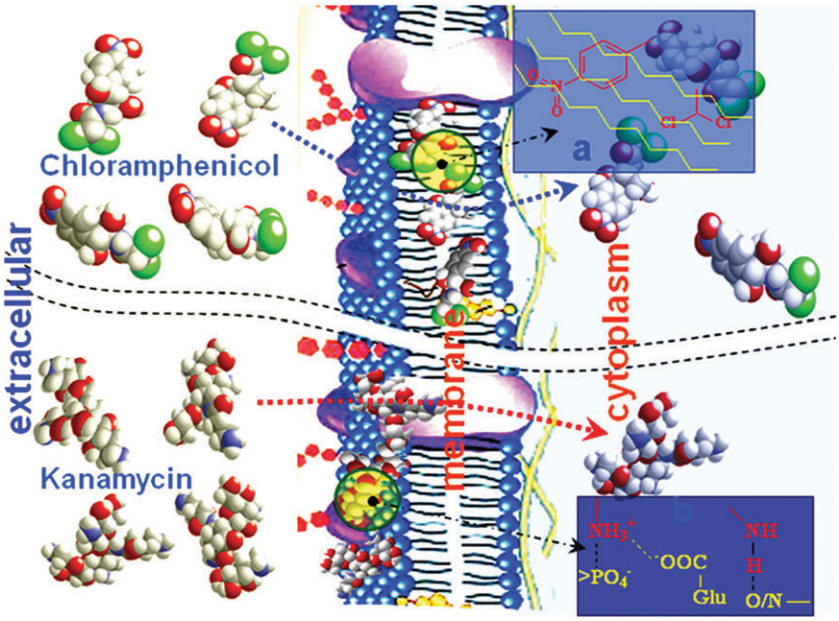

Fig. 6 Illustration of the different membrane transport pathways of two antibiotics with different structures and polarities: path a, transmembrane behavior of chloramphenicol (CAP); path b, transmembrane behavior of kanamycin sulfate (KAN); a, CAP concentrated in the membrane; b, KAN concentrated on the outer side of the membrane.

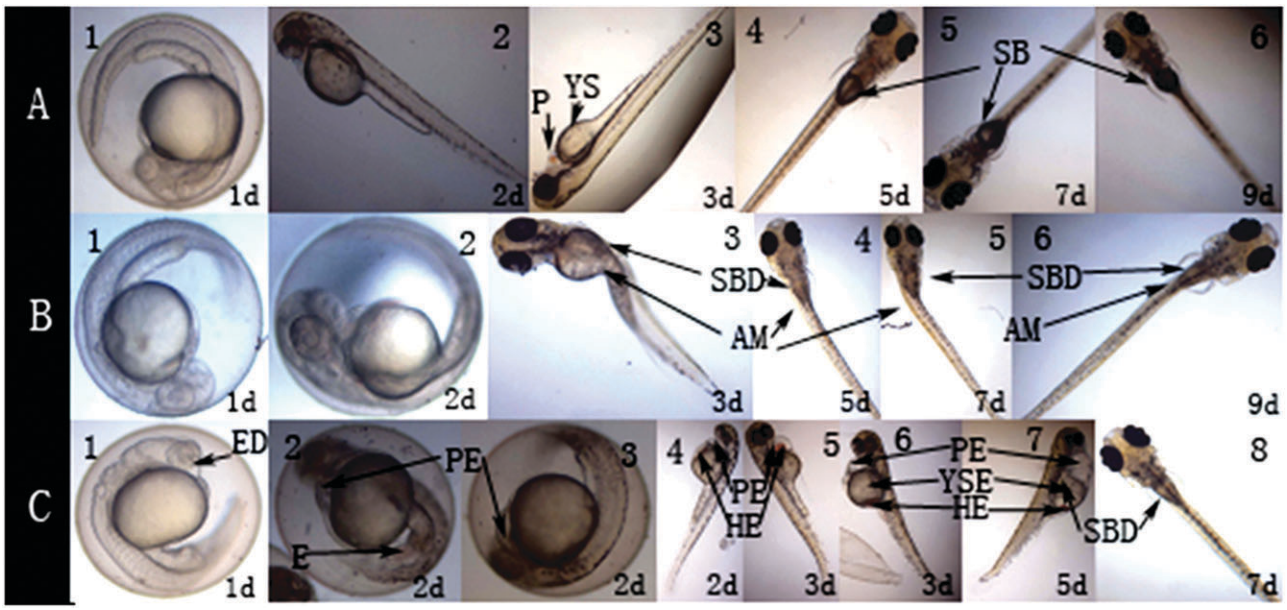

Fig. 7 Toxicity effects on zebrafish embryos and larvae. A, Controls showed normal developing embryos and larvae after exposure to the reconstituted buffer; B, KAN exposure groups (nominal exposure concentrations: 1–4, 6, 0.72 mM; 5, 1.44 mM); C, CAP exposure groups (nominal exposure concentrations: 1–2, 0.24 mM; 3–7, 0.12 mM; 8, 0.03 mM). AM, Axial malformation; E, Edema; ED, Eye deficit; HE, Hemagglutination; P, Pericardial; PE, Pericardial edema; SB, Swim bladder; SBD, Swim bladder defect; YS, Yolk sac; YSE, Yolk sac edema.

The median lethal concentration (LC_{50}) was calculated from the embryo and larva mortality rates. The 24 h LC_{50} for KAN was more than 5.76 mM for embryos and 3.50 mM for larvae, while the corresponding values for CAP were 0.34 mM and 0.68 mM, respectively. Thus, the larvae are more sensitive to KAN than the embryos but the converse for CAP. It supports the view that KAN causes physical damage with short-term effects while CAP mainly causes chemical damage with long-term effects. These characteristics of the antibiotics are closely related to the mechanisms of toxicity. KAN was mainly enriched in the outer chorion surface, so it failed to kill the embryos at 5.76 mM even at the 3rd day because of the protection of chorion (Fig. 8A), but it directly caused the larvae death only for one day exposure (ESI†, Fig. S8A). However, the enrichment of KAN on the outer chorion surface may prevent nutrient absorption and affect embryo

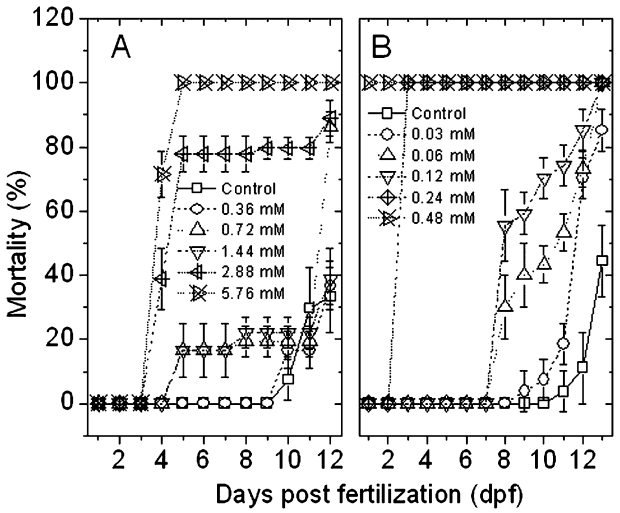

Fig. 8 Mortality of zebrafish embryos and larvae after exposure to different concentrations of kanamycin sulfate (KAN) or chloramphenicol (CAP) to evaluate the acute and chronic toxicities of the antibiotics: (A) KAN exposure group; (B) CAP exposure group.

development, reducing the percentage hatched and prolonging the hatching time. CAP passed through the membrane readily and may bind to serum albumin[42] and enzyme[68] in the blood circulation system, affecting metabolism and causing serious deformities (Fig. 7C; ESI†, Fig. S7B).

Conclusions

Zebrafish embryos were exposed to two structurally different antibiotics: KAN and CAP. The KAN binding was consistent with the general Langmuir adsorption isotherm while the CAP binding conformed to a general model of partitioning behavior. They exhibited different transmembrane distributions. More than 89% of the adsorbed KAN was located on the outer chorion surface, while over 80% of the adsorbed CAP entered the internal matrix of the chorion. They caused different toxic effects, too. KAN may cause physical damage of embryo membrane *e.g.* leading to delay of hatching and AM, but CAP transfer to the developing embryo *e.g.* causing serious deformities in the cardiovascular system. This method established could be used to elucidate the interactions of toxins with membranes and be helpful in toxicological research of chemicals.

Experimental

Apparatus and materials

The concentration of CAP was determined by high performance liquid chromatography (HPLC) (Model L-2000, Hitachi, Japan) using an L-2130 pump, a diode array detector (DAD) (Model L-2455), an inverse-phase column (C_{18}, Model Allsphere ODS-2 5u, 250 mm × 4.6 mm, Alltech Associates, Inc., USA). The purity of PC and KAN concentration was determined using HPLC with an evaporative light scattering detector (ELSD) (ELSD-UM3000, Tianjin Watson Analytical Instruments Co., Ltd, China). A freeze-dryer (Model K750X, Jintan Etong Electrons, China) was used to prepare lyophilized embryos, and changes in the 3-D morphology of the outer chorion surface were examined using a scanning electron microscopy (SEM) (Model S-4800, Hitachi Inc., Japan). An ultrasonic cell disruptor (Model JY92-II, Ningbo Scientz Biotechnology Co., Ltd, China) was used to disperse the embryos. A high-speed centrifuge (Model TG16-WS, Changsha Xiangyi Centrigufe Instrument Co., Ltd, China) was used to separate the membranes and cytoplasm. A vibrating thermostat (Model CHA-2, Jintan Etong Electrons, China) was used to maintain temperature and ensure that the suspensions remained thoroughly mixed during antibiotic exposure. A Model pH S-25 Acidity Meter (Shanghai Precise Instruments., China) was used to measure pHs. An ultrasonic cleaning device (Model SK3300H, Shanghai Ultrasonic Cleaning Instruments, China) was used to accelerate the dispersion of PC. An inverted microscope (Model TE2000-U, Nikon Inc., Japan) with a charge-coupled device (CCD) (Evolution^{TM} MP, Media Cybernetics, Japan) and digital photomicrography computer software (Image-Pro *Plus* 6.0) was used to observe toxicity-related changes in the zebrafish embryos and larvae.

Lecithin (CAS 8002-43-5 and Product No. 69014933) was purchased from Sinopharm Chemical Reagent Co., Ltd, China. The standard substances of PEA (CAS 39382-08-6 and Product No. P7943) and PC (CAS 8002-43-5 and Product No. P3556) were purchased from Sigma-Aldrich and their contents in lecithin determined by HPLC-ELSD using a normal-phase column (Luna 5 μ Silica (2) 100 A, 5 μm, 250 × 4.60 mm, Phenomenex, USA).[50] All organic solvents were HPLC grade solvents. Hexane (CAS 110-54-3 and Lot No.10010001) and isopropanol (CAS 67-63-0 and Lot No. 08050003) were obtained from Sinopharm Chemical Reagent Co., Ltd, China. Trifluoroacetic acid (CAS 76-05-1 and Lot No.802231) was obtained from Tedia company, inc., USA. Methanol (CAS 67-56-1 and Product No.1060074000) was obtained from Merck KGaA, Germany. 20 g L^{-1} of lecithin was suspended in deionized water and dispersed ultrasonically at maximal amplitude at 4 °C for 5 cycles of 15 s interspersed with 45 s periods of rest.[63] The SML suspension was thus formed and used to simulate antibiotic interactions *in vitro*. Carrez I solution was prepared by dissolving 15 g $K_4[Fe(CN)_6]\cdot 3H_2O$ in 100 mL deionized water, and Carrez II solution by dissolving 30 g $ZnSO_4\cdot 7H_2O$ in 100 mL deionized water.[69] These were used to co-precipitate SML. Britton-Robinson (BR) buffers at pH 4.5, 5.5, 6.5, 7.5 and 8.5 were prepared to investigate the pH effect, a series of NaCl concentrations (0, 0.10, 0.15, 0.20, 0.25 M) was used to examine the effects of electrolyte, and different temperatures (15, 25, 35, 45, 55 °C) were set using the thermostat vibrator to examine temperature effects. In the pH, temperature and electrolyte experiments, a factor varied and the other two factors were fixed where the conditions were temperature at 25 °C, pH at 7 and no electrolyte added. Reconstituted buffer (ISO 6341) was prepared by mixing 0.294 g $CaCl_2\cdot 2H_2O$, 0.123 g $MgSO_4\cdot 7H_2O$, 0.065 g $NaHCO_3$ and 0.006 g KCl in 1000 mL deionized water and was ventilated close to 100% oxygen saturation with aquarium air-pump (Model ACO-5503, Guangdong Hailea Group, China). Stock solutions of 8.00 mM KAN and 6.00 mM CAP (Sigma-Aldrich. Inc., USA) were

prepared in deionized water, then diluted daily to the concentrations used for exposure.

Adsorption of KAN and CAP on SML

KAN or CAP was mixed with SML in 10.0 mL deionized water. The concentration of KAN ranged from 0.1 to 1.5 mM and of CAP from 60 to 1500 mg L^{-1}; PC concentration was 1.14 mM. After the mixture was incubated for 1 h, 0.10 mL Carrez I and 0.10 mL Carrez II were added to them. The liquid was mixed thoroughly and centrifuged for 10 min at 12 000 rpm. The concentration of KAN in the supernatants was determined by HPLC with the ELSD detector[70] using a C_{18} chromatographic column (Allsphere ODS-2 5u). Chromatographic conditions for determining the concentration of KAN using the HPLC-ELSD are as follows: the optimized mobile phase was water–methanol (95 : 5 v/v) with 0.2 mM trifluoroacetic acid in water, the flow rate was 1.0 mL min^{-1} (isocratic mode), the nitrogen pressure was 3.27 bar and the evaporation temperature was 60 °C. The concentration of CAP was determined by HPLC using a DAD detector[71] and the C_{18} chromatographic column. Chromatographic conditions for determining the concentration of CAP using the HPLC-DAD are as follows: the mobile phase was methanol–water (55 : 45, v/v), the flow rate was 1.0 mL min^{-1}, the column temperature was set at 25 °C and the measurement wavelength at 278 nm. All injections (20.0 μL) were performed manually. KAN was eluted at 3.1 min (ESI†, Fig. S2A) and CAP at 3.5 min (ESI†, Fig. S2B). Each test was replicated three times consecutively.

Cultivation, collection and exposure of embryos

The parental zebrafish were kept in a 25 L tank with the following control settings: 250 mg L^{-1} hardness (calculated as $CaCO_3$), pH 7.5 ± 0.5, 10.5 ± 0.5 mg L^{-1} dissolved oxygen. The photoperiod was adjusted to a 14/10 h light/dark cycle at 26 ± 1 °C. The fish were fed regularly with frozen red mosquito larvae from an uncontaminated source. Before any tests were performed, several spawning boxes (12 × 20 × 12 cm) each containing a mesh (3–4 mm gap) were placed in a tank with six male and three female fish in each box. Spawning and fertilization took place within 30 min under light illumination. The fertilized eggs were collected and rinsed with reconstituted buffer, which had been ventilated close to 100% oxygen saturation. Normally developing embryos were selected under an inverted microscope. To ensure that the experiments gave valid results, fertilized eggs were obtained only from spawns with a fertilization rate higher than 90%. Two hpf embryos and 2 h post-hatching (hph) larvae were used for exposure.

Fragmentation of embryos and determinations of KAN and CAP

In the membrane transport experiments, KAN (0.90, 1.80, 2.70, 3.60 and 4.50 mM) and CAP (80, 160, 320, 640 and 960 mg L^{-1}) were used for embryo exposures. Twenty embryos were incubated (a) in 5.0 mL KAN or CAP solutions for 8 h (ESI†, Fig. S5 1), then the concentration of excess antibiotic in the supernatants (c_{L1}) was determined (ESI†, Fig. S5 2). All embryos were separated (ESI†, Fig. S5 3) and rinsed with deionized water, then suspended (b) in 3 mL deionized water (ESI†, Fig. S5 4) and ultrasonicated (c) for 10 × 5 s at 120 w interspersed with 5 s intervals of rest. The mixture (ESI†, Fig. S5 5) was centrifuged (d) for 5 min at 6000 rpm. The supernatant containing cytoplasm was diluted to 5 mL (ESI†, Fig. S5 6) with deionized water and the antibiotic content (c_{L2}) was determined. The membrane pellet (ESI†, Fig. S5 7) was suspended (b) in 1 mL dichloromethane (ESI†, Fig. S5 8) and ultrasonicated (c) for 90×30 s at 240 w interspersed with 15 s intervals of rest. The mixture (ESI†, Fig. S5 9) was centrifuged (d) for 10 min at 12 000 rpm, the supernatant was diluted to 5 mL with methanol (ESI†, Fig. S5 10), and the antibiotic content (c_{L3}) was determined. Membranes free of antibiotics remained in the pellet (ESI†, Fig. S5 11). The antibiotic concentrations (c_{L1}, c_{L2}, c_{L3}) were determined by HPLC and the molar amounts of KAN or CAP (γ_{KAN} or [CAP]) bound to SML, embryos and different parts of the embryos (extracellular, membrane and cytoplasm) were calculated. Each test was replicated three times consecutively.

3D-morphology of the embryo surface

Five embryos were exposed to 4.00 mM KAN or 2.00 mM CAP. After incubation for 8 h, the supernatant was removed and the embryos were freeze-dried for 12 h at −55 °C. The 3D-morphology of the lyophilized embryos was observed using SEM and photographs were captured in the presence of KAN and CAP. Using the same method, a control sample not exposed to antibiotics was incubated and observed in order to compare the chorion surfaces.

Toxicity of KAN and CAP

The embryos were exposed to KAN- and CAP-containing media, and 25 mL glass petri dishes were used as test chambers for toxicity bioassays. Ten embryos were exposed to 10.0 mL of the solution and incubated at 26 ± 0.5 °C under a 14 h light/10 h dark photoperiod; the concentrations of KAN were 0.36, 0.72, 1.44, 2.88 and 5.76 mM and those of CAP were 0.03, 0.06, 0.12, 0.24 and 0.48 mM. A reference control was prepared with the reconstituted buffer instead of antibiotics. Photographs showing the toxic effects on embryos and larvae were obtained at 1–13 dpf with an inverted microscope and the images were compared among the control group, KAN exposure groups and CAP exposure groups. Death was defined by cessation of heart beat or coagulation of the embryos and the mortality rates of the embryos and larvae were calculated. Dead embryos and larvae were removed promptly from the petri dishes. The LC_{50} for the embryos and larvae were calculated by probit analysis. Each test was replicated three times consecutively.

Abbreviations

AM	axial malformation
BR	Britton-Robinson
CAP	chloramphenicol
CCD	charge-coupled device
CMC	critical micelle concentration
DAD	diode array detector
DDPC	dipalmitoylphosphatidylcholine

ELS	early life stage
ELSD	evaporative light scattering detector
HE	hemoglutination
h(d)pf	hours (days) post fertilization
h(d)ph	hours (days) post hatching
HPLC	high performance liquid chromatography
KAN	kanamycin
LC_{50}	median lethal concentration
PC	phosphatidylchline (lecithin)
PE	pericardial edema
PEA	phosphatidylethanolamine
PPCPs	pharmaceuticals and personal care products
SML	single membrane liposome
SEM	scanning electron microscope
TP	palmitic acid triglyceride
YSE	yolk sac edema

Acknowledgements

This work was supported by the funds of the National 973 Project of China (Grant No. 2010CB912604) and the National S&T Major Project of China (Grant No.2008ZX07421-002).

References

1 A. B. A. Boxall, L. A. Fogg, P. A. Blackwell, P. Kay, E. J. Pemberton and A. Croxford, *Rev. Environ. Contam. Toxicol.*, 2004, **180**, 1–91.
2 F. C. Cabello, *Environ. Microbiol.*, 2006, **8**, 1137–1144.
3 A. K. Sarmah, M. T. Meyer and A. B. A. Boxall, *Chemosphere*, 2006, **65**, 725–759.
4 D. G. Capone, D. P. Weston, V. Miller and C. Shoemaker, *Aquaculture*, 1996, **145**, 55–75.
5 I. Robinson, G. Junqua, R. Van Coillie and O. Thomas, *Anal. Bioanal. Chem.*, 2007, **387**, 1143–1151.
6 G. Rigos, I. Nengas, M. Alexis and G. M. Troisi, *Aquat. Toxicol.*, 2004, **69**, 281–288.
7 J. L. Martinez, *Science*, 2008, **321**, 365–367.
8 T. Heberer, *Toxicol. Lett.*, 2002, **131**, 5–17.
9 F. Gagne, C. Blaise and C. Andre, *Ecotoxicol. Environ. Saf.*, 2006, **64**, 329–336.
10 B. A. J. Kallen, P. O. Olausson and B. R. Danielsson, *Reprod. Toxicol.*, 2005, **20**, 209–214.
11 N. Hocaoglu, R. Atilla, F. Onen and Y. Tuncok, *Hum. Exp. Toxicol.*, 2008, **27**, 585–589.
12 L. Weinstein, T. L. Doan and M. A. Smith, *Am. J. Health-Syst. Pharm.*, 2009, **66**, 345–347.
13 J. H. Oh, H. J. Park, J. S. Lim, S. Y. Jeong, J. Y. Hwang, Y. Kim and S. Yoon, *Mol. Cell. Toxicol.*, 2006, **2**, 185–192.
14 A. K. Karabulut, I. I. Uysal, H. Acar and Z. Fazliogullari, *Anatomia Histologia Embryologia*, 2008, **37**, 369–375.
15 H. Sumano, L. Gutierrez, C. Velazquez and S. Hayashida, *Acta Veterinaria Hungarica*, 2005, **53**, 231–240.
16 J. M. Kim, J. R. Ha, S. W. Oh, H. G. Kim, J. M. Lee, B. O. Kim, D. G. Lee, S. H. Lee and J. G. Kim, *J. Microbiol. Biotechnol.*, 2008, **18**, 1768–1772.
17 V. Naidoo and G. E. Swan, *Comp. Biochem. Phys. C*, 2009, **149**, 269–274.
18 S. M. Richards and S. E. Cole, *Ecotoxicology*, 2006, **15**, 647–656.
19 M. D. Yow and N. E. Tengg, *J. Pediatr.*, 1961, **58**, 538–547.
20 H. Umezawa, M. Ueda, K. Maeda, K. Yagishita, S. Kondo, Y. Okami, R. Utahara, Y. Osato, K. Nitta and T. Takeuchi, *J. Antibiot.*, 1957, **10**, 181–188.
21 M. Hainrichson, I. Nudelman and T. Baasov, *Org. Biomol. Chem.*, 2008, **6**, 227–239.
22 Y. Toyoda and M. Tachibana, *Acta Oto-Laryngologica*, 1978, **86**, 9–14.
23 Y. Shimizu, H. Hakuba, J. Hyodo, M. Taniguchi and K. Gyo, *Neurosci. Lett.*, 2005, **380**, 243–246.
24 L. Yu, H. Tang and H. C. Chan, *Cell Biol. Int.*, 2008, **32**, S47–S47.
25 Z. Y. Huang, M. Y. Sun, S. Li and G. L. Huang, *Aquacult. Res.*, 2006, **37**, 1540–1545.
26 S. P. Ho, T. Y. Hsu, M. H. Chen and W. S. Wang, *J. Vet. Med. Sci.*, 2000, **62**, 479–485.
27 I. Uriarte, A. Farias and J. C. Castilla, *Aquacult. Eng.*, 2001, **25**, 139–147.
28 A. I. Campa-Córdova, A. Luna-Gonzalez, F. Ascencio, E. Cortes-Jacinto and C. J. Caceres-Martinez, *Aquaculture*, 2006, **260**, 145–150.
29 D. E. Holt, T. A. Ryder, A. Fairbairn, R. Hurley and D. Harvey, *Hum. Exp. Toxicol.*, 1997, **16**, 570–576.
30 D. E. Holt, C. M. Andrews, J. P. Payne, T. C. Williams and J. A. Turton, *Hum. Exp. Toxicol.*, 1998, **17**, 8–17.
31 C. T. Kong, D. E. Holt, S. K. Ma, A. K. W. Lie and L. C. Chan, *Hum. Exp. Toxicol.*, 2000, **19**, 503–510.
32 Z. Abbas, I. Malik and A. Khan, *J. Pak. Med. Assoc.*, 1993, **43**, 58–59.
33 S. Robbana-Barnat, F. Decloitre, C. Frayssinet, J. M. Seigneurin, L. Toucas and C. LafargeFrayssinet, *Drug Chem. Toxicol.*, 1997, **20**, 239–253.
34 A. Schmittgraff, *Acta Haematol.*, 1981, **66**, 267–268.
35 C. R. Suarez and E. P. Ow, *Pediatr. Cardiol.*, 1992, **13**, 48–51.
36 M. Gweba, K. I. Onifade and O. O. Faleke, *Int. J. Pharmacol.*, 2009, **5**, 76–80.
37 M. O. Oyeyemi and D. A. Adeniji, *Int. J. Morphol.*, 2009, **27**, 7–11.
38 S. Sánchez-Fortún, F. Marva, M. Rouco, E. Costas and V. Lopez-Rodas, *Ecotoxicology*, 2009, **18**, 481–487.
39 L. Li, H. W. Gao, J. R. Ren, L. Chen, Y. C. Li, J. F. Zhao, H. P. Zhao and Y. Yuan, *BMC Struct. Biol.*, 2007, **7**, 16, DOI: 10.1186/1472-6807-7-16.
40 H. W. Gao, Q. Xu, L. Chen, S. L. Wang, Y. Wang, L. L. Wu and Y. Yuan, *Biophys. J.*, 2008, **94**, 906–917.
41 F. F. Chen, Y. N. Tang, S. L. Wang and H. W. Gao, *Amino Acids*, 2009, **36**, 399–407.
42 F. Ding, G. Y. Zhao, S. C. Chen, F. Liu, Y. Sun and L. Zhang, *J. Mol. Struct.*, 2009, **929**, 159–166.
43 L. L. Wu, H. W. Gao, N. Y. Gao, F. F. Chen and L. Chen, *BMC Struct. Biol.*, 2009, **9**, 31, DOI: 10.1186/1472-6807-9-31.
44 L. L. Wu, L. Chen, C. Song, X. W. Liu, H. P. Deng, N. Y. Gao and H. W. Gao, *Amino Acids*, 2010, **38**, 113–120.
45 Z. Xu, X. W. Liu, Y. S. Ma and H. W. Gao, *Environ. Sci. Pollut. Res.*, 2010, **17**, 798–806.
46 T. Siibak, L. Peil, L. Q. Xiong, A. Mankin, J. Remme and T. Tenson, *Antimicrob. Agents Chemother.*, 2009, **53**, 563–571.
47 H. T. Lai, J. H. Hou, C. I. Su and C. L. Chen, *Ecotoxicol. Environ. Saf.*, 2009, **72**, 329–334.
48 R. Nagel, *Altex-Altern. Tierexp.*, 2002, **19**, 38–48.
49 F. Lahnsteiner, *Atla-Altern. Lab. Anim.*, 2008, **36**, 299–311.
50 H. A. Wu, X. H. Mai and R. R. Hu, *Academ. J. Guangdong College Pharm.*, 2003, **19**, 228–229.
51 J. X. Yang, H. W. Gao, Z. J. Hu and M. H. Jiang, *J. AOAC int.*, 2005, **88**, 866–872.
52 I. Langmuir, *J. Am. Chem. Soc.*, 1918, **40**, 1361–1403.
53 A. Leo, C. Hansch and D. Elkins, *Chem. Rev.*, 1971, **71**, 525–616.
54 M. Switala, R. Hrynyk, A. Smutkiewicz, K. Jaworski, P. Pawlowski, P. Okoniewski, T. Grabowski and J. Debowy, *J. Vet. Pharmacol. Ther.*, 2007, **30**, 145–150.
55 P. Sapia, L. Coppola, G. Ranieri and L. Sportelli, *Colloid Polym. Sci.*, 1994, **272**, 1289–1294.
56 H. I. Petrache, T. Zemb, L. Belloni and V. A. Parsegian, *Proc. Natl. Acad. Sci. U. S. A.*, 2006, **103**, 7982–7987.
57 A. S. Ulrich, *Biosci. Rep.*, 2002, **22**, 129–150.
58 M. R. Moncelli, L. Becucci and R. Guidelli, *Biophys. J.*, 1994, **66**, 1969–1980.
59 T. Shitara, E. Umemura, T. Tsuchiya and T. Matsuno, *Carbohydr. Res.*, 1995, **276**, 75–89.
60 A. P. Vanwezel and A. Opperhuizen, *Chemosphere*, 1995, **31**, 3605–3615.
61 P. J. Rombough, *Comp. Biochem. Physiol., Part C: Pharmacol., Toxicol. Endocrinol.*, 1985, **82**, 115–117.
62 J. Sikkema, J. A. M. Debont and B. Poolman, *J. Biol. Chem.*, 1994, **269**, 8022–8028.

63 K. Saar, M. Lindgren, M. Hansen, E. Eiriksdottir, Y. Jiang, K. Rosenthal-Aizman, M. Sassian and U. Langel, *Anal. Biochem.*, 2005, **345**, 55–65.
64 B. D. van Rooijen, M. M. A. E. Claessens and V. Subramaniam, *Biochim. Biophys. Acta, Biomembr.*, 2009, **1788**, 1271–1278.
65 Y. Sokolov, J. A. Kozak, R. Kayed, A. Chanturiya, C. Glabe and J. E. Hall, *J. Gen. Physiol.*, 2006, **128**, 637–647.
66 R. R. Fripp, M. C. Carter, J. C. Werner, H. G. Schuler, A. M. Rannels, V. Whitman and N. M. Nelson, *J. Pediatr.*, 1983, **103**, 487–490.
67 T. Biancaniello, R. A. Meyer and S. Kaplan, *J. Pediatr.*, 1981, **98**, 828–830.
68 F. Ding, G. Y. Zhao, J. L. Huang, Y. Sun and L. Zhang, *Eur. J. Med. Chem.*, 2009, **44**, 4083–4089.
69 V. Gokmen, H. Z. Senyuva, J. Acar and K. Sarioglu, *J. Chromatogr., A*, 2005, **1088**, 193–199.
70 N. C. Megoulas and M. A. Koupparis, *Anal. Chim. Acta*, 2005, **547**, 64–72.
71 H. X. Chen, H. Chen, J. Ying, J. L. Huang and L. Liao, *Anal. Chim. Acta*, 2009, **632**, 80–85.

